

The $\Lambda_Q\Lambda_Q$ Potential

Daniel Arndt^a, Silas R. Beane^b and Martin J. Savage^a

^a *Department of Physics, University of Washington,
Seattle, WA 98195.*

^b *Institute for Nuclear Theory, University of Washington,
Seattle, WA 98195.*

Abstract

Lattice QCD simulations of the potential between two baryons, each containing a heavy quark and two light quarks, such as the $\Lambda_Q\Lambda_Q$ potential, will provide insight into the nucleon-nucleon interaction. As one-pion exchange does not contribute to the $\Lambda_Q\Lambda_Q$ potential, the long-distance behavior is dominated by physics that contributes to the intermediate-range attraction between two nucleons. We compute the leading long-distance contributions to the $\Lambda_Q\Lambda_Q$ potential in QCD and in partially-quenched QCD in the low-energy effective field theory.

arXiv:nucl-th/0304004v1 1 Apr 2003

April 2003

I. INTRODUCTION

The nucleon-nucleon (NN) potential has been studied for many decades, and modern NN potentials have been constructed to reproduce all NN scattering data below ~ 500 MeV to very-high precision [1]. It is well established that the long-distance component of the potential is due to one-pion exchange (OPE). A clear demonstration of this point is provided in work by the Nijmegen group where the charged and neutral pion masses are free parameters in the OPE component that are fit to the NN phase-shift data [2]. The fit values of the masses reproduce with high accuracy the physical values of the pion masses. Somewhat more controversial are the intermediate-range and short-range components of the NN potential. In the simplest potentials based on one-meson exchange (OME) the intermediate-range attraction is supplied by the exchange of the (fictitious) “ σ ”-meson, while the short-range repulsion is supplied by the exchange of the ρ and ω mesons. In modern potentials, such as the AV₁₈ potential, the intermediate- and short-range components of the NN potential are not assumed to arise from the exchange of a single meson and *ad hoc* smooth functions are used to best reproduce the NN phase-shift data [1]. The last decade has seen considerable progress towards formulating NN interactions and multi-nucleon interactions in an effective field theory (EFT) consistent with the approximate chiral symmetry of QCD [3]. In fact, recently it was shown that an NN potential computed with the EFT better reproduces the NN scattering data than the potentials based on OME [4]. More precisely, the two-pion exchange (TPE) component of the potential provides a better description of the intermediate-range component than the exchange of a “ σ ”-meson [4]. Further it was shown that the extracted values of coefficients of one-nucleon local operators in the chiral Lagrangian that gives rise to the potential are consistent with their determination in the πN sector [4]. This strongly suggests that the intermediate-distance components of the NN potential can be described by the exchange of uncorrelated pions with interactions constrained by chiral symmetry. This is a very encouraging situation, as ultimately one wants to make a direct and quantitative connection between QCD and nuclear physics using the language of effective field theory [3].

It is through lattice QCD simulations that definitive predictions in nuclear physics will be made directly from QCD. Given the current state of technology, simulations of multi-nucleon systems are intractable, but realistic simulations of two-nucleon systems are presently feasible. Arguably, the most promising method is to calculate scattering phase shifts directly using Lüscher’s finite-volume algorithm, which, for instance, expresses the ground-state energy of a two-particle state as a perturbative expansion in the scattering length divided by the size of the box [5]. This method has been used successfully to study $\pi\pi$ scattering [6]. There has also been an attempt to compute NN scattering parameters in lattice QCD; Ref. [7] computes the S-wave scattering lengths in quenched QCD (QQCD) using Lüscher’s method.

A second approach to the NN system on the lattice is to study the simplified problem of two interacting heavy-light particles [8–13]. It has been suggested that lattice QCD simulations of the potential between hadrons containing a heavy quark will provide insight into the nature of the intermediate-range force between two nucleons [14]. In the heavy-quark limit, the kinetic energy of the heavy hadrons is absent and the lowest-lying energy eigenvalues, which can be measured on the lattice, are given by the interaction potential. To our knowledge, all discussions to date have addressed two heavy mesons, say BB . This

case is somewhat complicated by the fact that B and B^* are degenerate in the heavy-quark limit and therefore require a coupled-channel analysis. In this work we consider the $\Lambda_Q\Lambda_Q$ interaction (where the Λ_Q is the lowest-lying baryon containing one heavy quark, Q), which does not suffer from this complication, and we compute the leading contribution to the $\Lambda_Q\Lambda_Q$ potential in the chiral expansion. Since the Λ_Q is an isosinglet, there is no OPE, and the leading large-distance behavior is governed by TPE, which is physics analogous to the intermediate-range attraction in the NN potential.

Presently, unquenched lattice simulations with the physical values of the light-quark masses are prohibitively time-consuming, even on the fastest machines. While some quenched calculations can be performed with the physical quark masses there is no limit in which they reproduce QCD, and consequently they should be considered to be a warm-up exercise for the “real thing”. Relatively recently it was realized that partially-quenched (PQ) simulations, in which the sea quarks are more massive than the valence quarks, provide a rigorous way to determine QCD observables and are less time-consuming than their QCD counterparts. It is with PQ simulations that nuclear-physics observables will first be calculated rigorously from QCD. As PQQCD reproduces QCD only in the limit in which the sea-quark masses become equal to the valence-quark masses which, in turn, are set equal to the physical values of the light quark masses (we call this the QCD limit), there are some interesting features of the PQ theory that are distinct from nature away from the QCD limit. In QCD, the long-distance component of the NN potential is due to OPE, as discussed above. However, in PQQCD there is also a contribution from the exchange of the η -meson (in the theory with two flavors of light quarks). In QCD such an exchange is suppressed due to the large mass of the η compared to the π . However, in PQQCD the η propagator has a double-pole component that depends on the pion mass due to the hairpin interactions with a coefficient that depends upon the difference between the masses of the sea and valence quarks. Therefore, away from the QCD limit the long-distance component of the NN potential is dominated by one-eta exchange (OEE) and falls exponentially with a range determined by the pion mass, $\sim e^{-m_\pi r}$, as opposed to the familiar Yukawa type behavior [15]. This exponential behavior is even more pronounced in quenched calculations. Therefore, it is likely that quenched and PQ calculations of the NN potential will unfortunately be dominated by quenching and partial-quenching artifacts. While this seems like a negative state-of-affairs, there is hope that the PQ simulations will tell us something about the NN interaction. An EFT with consistent power-counting describing the multi-nucleon sector [16] has recently been developed, and its partially-quenched counterpart was straightforwardly constructed [17]. The NN scattering amplitudes in the S-waves were computed out to next-to-leading order (NLO) in the EFT power-counting, while the contributions to the higher partial waves, resulting from OPE and OEE, were computed at leading order. The hope is that finite-volume lattice calculations [5] can be performed to extract the NN phase-shifts directly from PQQCD through the use of the scattering amplitudes computed in Ref. [17]. Unfortunately, given the violence that quenching and partial-quenching do to the long-distance component of the NN potential, there is little hope that such calculations can shed light on the nature of the intermediate-range component of the NN force.

II. THE $\Lambda_Q\Lambda_Q$ POTENTIAL IN QCD

The lowest-lying baryons containing a single heavy quark can be classified by the spin of their light degrees of freedom (dof), s_l , in the heavy-quark limit, $m_Q \rightarrow \infty$. Working with two light flavors, u and d quarks, the light dof of the isosinglet baryon, Λ_Q , have $s_l = 0$, while the light dof of the isotriplet baryons, $\Sigma_Q^{\pm 1,0}$ and $\Sigma_Q^{\pm 1,0*}$, (the superscript denotes the third component of isospin) have $s_l = 1$ ¹. In the heavy-quark limit the spin- $\frac{1}{2}$ $\Sigma_Q^{\pm 1,0}$ baryons are degenerate with the spin- $\frac{3}{2}$ $\Sigma_Q^{\pm 1,0*}$ baryons, but are split in mass from the Λ_Q by an amount that does not vanish in the chiral limit. The Lagrange density describing the interactions of these heavy baryons with the pions is [18,19]

$$\begin{aligned} \mathcal{L} = & i\bar{\Lambda}_Q v \cdot D\Lambda_Q - i\bar{S}_\mu^{ij} v \cdot DS_\mu^{ij} + \bar{\Delta}\bar{S}_\mu^{ij} S_\mu^{ij} + ig_2\epsilon_{\mu\nu\sigma\lambda}\bar{S}^{\mu,ij}v^\nu(A^\sigma)_i^k S_{jk}^\lambda \\ & + g_3\left(\bar{\Lambda}_Q\epsilon^{ij}(A_\mu)_i^k S_{jk}^\mu + \text{h.c.}\right) \quad , \end{aligned} \quad (1)$$

where S_{ij}^μ is the superfield containing both the $\Sigma_Q^{\pm 1,0}$ and $\Sigma_Q^{\pm 1,0*}$, $A_\mu = \frac{i}{2}(\xi\partial_\mu\xi^\dagger - \xi^\dagger\partial_\mu\xi)$ is the axial-vector field of pions, v_μ is the heavy-hadron four-velocity, $g_{2,3}$ are coupling constants that must be determined either from data or from lattice QCD, and $\bar{\Delta}$ is the $\Sigma_Q^{(*)} - \Lambda_Q$ mass splitting in the heavy-quark limit. Experimentally, the measured width of the Σ_c^{*++} is $\Gamma(\Sigma_c^{*++}) = 17.9_{-3.2}^{+3.8} \pm 4.0$ MeV [20], which fixes the axial coupling g_3 to be $|g_3| = 0.95 \pm 0.08 \pm 0.08$ in the charmed sector. Recently, it has been conjectured that in QCD, $g_3 = 1$ and $g_2 = 2$ in the chiral limit [21]. The coupling g_2 might be measured through the radiative decays of the $\Sigma_c^{(*)}$ [22].

As the light dof in the Λ_Q have $s_l = 0$ in the heavy-quark limit, the light-quark axial current matrix element vanishes, and thus there is no $\Lambda_Q\Lambda_Q\pi$ interaction at leading order in the heavy quark expansion. This means that there is no OPE (or OEE) contribution to the $\Lambda_Q\Lambda_Q$ potential in QCD and PQCD, and therefore there is no long-distance component in the $\Lambda_Q\Lambda_Q$ potential. It is the two-pion exchange box and crossed-box diagrams, as shown in Fig. 1, that provide the longest-distance interaction between two Λ_Q 's. In addition, there are local four- Λ_Q operators at the same order in the chiral expansion but such local interactions give coordinate-space delta-functions. Not only are such local interactions allowed, they are required to absorb the divergences arising in the box and crossed-box diagrams in Fig. 1. Analogous diagrams to those in Fig. 1 in the two-nucleon sector provide part of the intermediate-range component of the NN potential. However, it is important to realize that there are additional interactions that contribute to the intermediate-range component of the NN potential in the chiral expansion, for instance contributions from the Weinberg-Tomazawa term and also from higher-dimension $\bar{N}N\pi\pi$ vertices. Therefore, while the $\Lambda_Q\Lambda_Q$ potential provides a window into the nature of the intermediate-range NN interaction, it certainly does not provide a complete description.

If the Λ_Q and $\Sigma_Q^{(*)}$ were degenerate, we would be required to solve the coupled-channel system with $\Lambda_Q\Lambda_Q$ and $\Sigma_Q^{(*)}\Sigma_Q^{(*)}$ coupled to $I = 0$. In the charmed sector the $\Sigma_c - \Lambda_c$ mass splitting is $\Delta = 167.1$ MeV and the $\Sigma_c^* - \Lambda_c$ mass splitting is $\Delta = 232.7$ MeV, and we use

¹For three light flavors the baryons fall into a $\mathbf{6} \oplus \bar{\mathbf{3}}$ of SU(3).

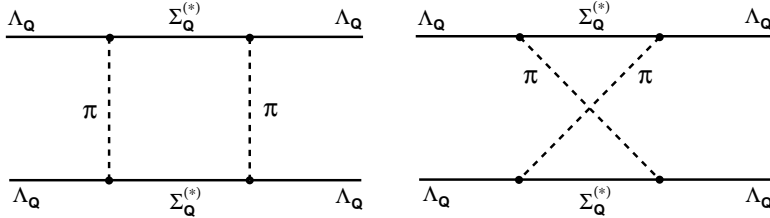


FIG. 1. The box and crossed-box diagrams that give the longest-distance component of the $\Lambda_Q\Lambda_Q$ potential. The vertices are taken from the Lagrangian in eq. (1). Heavy-quark symmetry forbids $\Lambda_Q\Lambda_Q$ intermediate states in the box and crossed-box diagrams.

the spin-weighted average of these splittings to estimate $\overline{\Delta} \sim 211$ MeV in the heavy-quark limit. There is no symmetry reason for this mass-splitting to vanish in the chiral limit, and hence there is no infrared divergence that requires a coupled-channel analysis. In the power-counting we treat $\overline{\Delta} \sim m_\pi$ and take the $M_{\Lambda_Q}, M_{\Sigma_Q} \rightarrow \infty$ limit in evaluating the diagrams in Fig. 1. With this power-counting, one can directly use the Feynman rules of Heavy-Baryon Chiral Perturbation Theory (HB χ PT) to describe the low-momentum dynamics of the nucleon and Δ -resonance, developed by Jenkins and Manohar [23], without the need to resum the baryon kinetic energy term as is the case for the box and crossed-box diagrams in the nucleon sector. Evaluating the diagrams in Fig. 1 and then Fourier transforming them to position space is straightforward. Using the integral representations of Ref. [24], the potential between two Λ_Q 's in QCD at leading order in the chiral expansion and in the isospin limit is

$$V^{\text{QCD}}(r) = -\frac{g_3^4}{8\pi^3 f_\pi^4 r^2} \int_0^\infty d\lambda \frac{\overline{\Delta}^2}{(\lambda^2 + \overline{\Delta}^2)^2} \mathcal{I}(\lambda, m_\pi, r) \quad , \quad (2)$$

where for notational simplicity we have defined the function $\mathcal{I}(\lambda, m, r)$ to be

$$\mathcal{I}(\lambda, m, r) = e^{-2r\sqrt{\lambda^2+m^2}} \left[2 \left(\lambda^2 + m^2 + \frac{3\sqrt{\lambda^2+m^2}}{r} + \frac{3}{r^2} \right)^2 + (\lambda^2 + m^2)^2 \right] \quad , \quad (3)$$

and $f_\pi \sim 132$ MeV. A useful feature of this integral representation is the separation between the $\overline{\Delta}$ and m_π dependence. The potential is shown in Fig. 2. For asymptotically large distances, the potential is well-approximated by

$$V^{\text{QCD}}(r) \rightarrow -\frac{3 g_3^4 m_\pi^{9/2}}{16 \pi^{5/2} r^{5/2} \overline{\Delta}^2 f_\pi^4} e^{-2m_\pi r} + \dots \quad , \quad (4)$$

which exhibits the expected fall off with a length scale set by twice the mass of the pion and where the dots represent subleading contributions in the large-distance expansion.

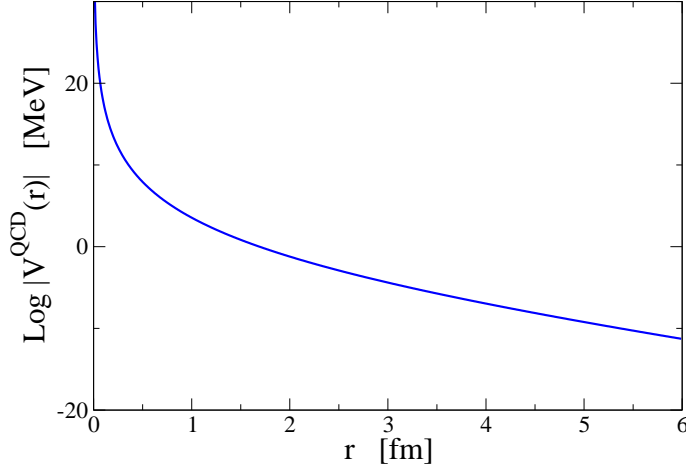


FIG. 2. The logarithm of the $\Lambda_Q\Lambda_Q$ potential in MeV as function of the distance between the Λ_Q in fm.

III. THE $\Lambda_Q\Lambda_Q$ POTENTIAL IN PQQCD

The extension of the heavy-baryon sector from QCD to PQQCD is straightforward². We use the notation and methods of Ref. [26]. To establish the representations of $SU(4|2)$ containing the Λ_Q and $\Sigma_Q^{(*)}$, we consider their interpolating fields. The interpolating field that contains the Λ_Q is

$$\mathcal{T}_{ij}^\gamma \sim \mathcal{Q}^{\gamma,c} \left[Q_i^{\alpha,a} Q_j^{\beta,b} + Q_j^{\alpha,a} Q_i^{\beta,b} \right] \epsilon_{abc} (C\gamma_5)_{\alpha\beta} \quad , \quad (5)$$

while the interpolating field that contains the Σ_Q 's is

$$\mathcal{S}_{ij}^{\gamma,\mu} \sim \mathcal{Q}^{\gamma,c} \left[Q_i^{\alpha,a} Q_j^{\beta,b} - Q_j^{\alpha,a} Q_i^{\beta,b} \right] \epsilon_{abc} (C\gamma^\mu)_{\alpha\beta} \quad , \quad (6)$$

where $Q_i^{\alpha,a}$ is a light-quark field operator with graded flavor index $i = 1, 2, \dots, 6$ where indices 1, 2, 3, 4 are fermionic and 5, 6 are bosonic. The other indices are the color index a and Dirac index α . The heavy-quark field operator is $\mathcal{Q}^{\gamma,c}$ that does not carry a graded flavor index. Under interchange of the light-quark flavor indices we find that

$$\mathcal{T}_{ij}^\gamma = (-)^{\eta_i\eta_j} \mathcal{T}_{ji}^\gamma \quad , \quad \mathcal{S}_{ij}^{\gamma,\mu} = (-)^{1+\eta_i\eta_j} \mathcal{S}_{ji}^{\gamma,\mu} \quad , \quad (7)$$

where $\eta_i = +1$ for fermionic indices and $\eta_i = 0$ for bosonic indices. It is then straightforward to show, following the techniques of Ref. [26], that the Λ_Q is embedded in a **17** dimensional representation of $SU(4|2)$, \mathcal{T}_{ij} , while the $\Sigma_Q^{(*)}$ are each embedded in a **19** dimensional representation of $SU(4|2)$, \mathcal{S}_{ij} . Under $SU(2)_q \otimes SU(2)_j \otimes SU(2)_{\bar{q}}$ the ground floor of level A

²The extension of the heavy-baryon sector to quenched QCD was carried out in Ref. [25]

of \mathcal{T}_{ij} transforms as a $(\mathbf{1}, \mathbf{1}, \mathbf{1})$ and contains the Λ_Q , the first floor of level A contains four baryons transforming as a $(\mathbf{2}, \mathbf{1}, \mathbf{2})$, while the ground floor of level B contains four baryons that transform as $(\mathbf{2}, \mathbf{2}, \mathbf{1})$. Similarly, the ground floor of level A of \mathcal{S}_{ij} transforms as a $(\mathbf{3}, \mathbf{1}, \mathbf{1})$ and contains the $\Sigma_Q^{(*)}$'s, the first floor of level A contains four baryons transforming as a $(\mathbf{2}, \mathbf{1}, \mathbf{2})$, while the ground floor of level B contains four baryons that transform as $(\mathbf{2}, \mathbf{2}, \mathbf{1})$. The remaining members of each irreducible representation do not contribute to the potential at the order we are working. The Lagrange density describing the dynamics of the lowest-lying baryons and the pseudo-Goldstone bosons is

$$\begin{aligned} \mathcal{L} = & i \left(\overline{\mathcal{T}} v \cdot D\mathcal{T} \right) - i \left(\overline{\mathcal{S}}^\mu v \cdot D\mathcal{S}_\mu \right) + \overline{\Delta} \left(\overline{\mathcal{S}}^\mu \mathcal{S}_\mu \right) \\ & + i g_2 \epsilon_{\mu\nu\sigma\lambda} \left(\overline{\mathcal{S}}^\mu v^\nu A^\sigma \mathcal{S}^\lambda \right) + \sqrt{2} g_3 \left(\overline{\mathcal{T}} A^\mu \mathcal{S}_\mu \right) \quad , \end{aligned} \quad (8)$$

where the covariant derivatives are

$$D_\mu \mathcal{T}_{ij} = \partial_\mu \mathcal{T}_{ij} + (V_\mu)_i^l \mathcal{T}_{lj} + (-)^{\eta_i(\eta_j + \eta_m)} (V_\mu)_j^m \mathcal{T}_{im} \quad , \quad (9)$$

and similarly for the \mathcal{S}^μ . The index contractions are

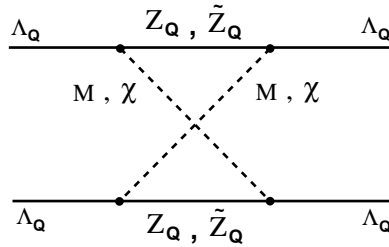


FIG. 3. Contributions to the crossed-box diagram from mesons and baryons containing ghost and sea quarks. The vertices are taken from the Lagrangian in eq. (8). The Z_Q are baryons containing one sea quark that transform as a $(\mathbf{2}, \mathbf{2}, \mathbf{1})$ under $SU(2)_q \otimes SU(2)_j \otimes SU(2)_{\bar{q}}$, while the \tilde{Z}_Q are baryons containing one ghost quark that transform as a $(\mathbf{2}, \mathbf{1}, \mathbf{2})$. The χ are fermionic mesons containing one ghost quark while the M are mesons containing one sea quark.

$$\begin{aligned} (\overline{\mathcal{T}} \Gamma \mathcal{T}) &= \overline{\mathcal{T}}^{\alpha,ji} \Gamma_\alpha^\beta \mathcal{T}_{\beta,ij} \quad , \quad (\overline{\mathcal{S}}^\mu \Gamma \mathcal{S}_\mu) = \overline{\mathcal{S}}^{\alpha\mu,ji} \Gamma_\alpha^\beta \mathcal{S}_{\beta\mu,ij} \\ (\overline{\mathcal{T}} \Gamma Y \mathcal{T}) &= \overline{\mathcal{T}}^{\alpha,ji} \Gamma_\alpha^\beta Y_i^l \mathcal{T}_{\beta,lj} \quad , \quad (\overline{\mathcal{S}}^\mu \Gamma Y \mathcal{S}_\mu) = \overline{\mathcal{S}}^{\alpha\mu,ji} \Gamma_\alpha^\beta Y_i^l \mathcal{S}_{\beta\mu,lj} \\ (\overline{\mathcal{T}} \Gamma Y^\mu \mathcal{S}_\mu) &= \overline{\mathcal{T}}^{\alpha,ji} \Gamma_\alpha^\beta (Y^\mu)_i^l \mathcal{S}_{\beta\mu,lj} \quad , \end{aligned} \quad (10)$$

where Γ acts on the Dirac indices and $Y \rightarrow UYU^\dagger$ acts in flavor space.

In PQQCD the box diagram in Fig. 1 is unmodified due to the fact that one cannot exchange two mesons containing either a ghost quark or a sea quark and have only two baryons (containing ghost and sea quarks) in the intermediate state. However, the crossed-box diagram is modified by quenching and partial quenching, as shown in Fig. 3. Writing the potential in PQQCD as $V^{\text{PQ}}(r) = V^{\text{QCD}}(r) + \delta V(r)$, we find that

$$\delta V(r) = + \frac{g_3^4}{48\pi^3 f_\pi^4 r^2} \int_0^\infty d\lambda \frac{\lambda^2 - \overline{\Delta}^2}{(\lambda^2 + \overline{\Delta}^2)^2} \left(\mathcal{I}(\lambda, m_{SV}, r) - \mathcal{I}(\lambda, m_\pi, r) \right) \quad , \quad (11)$$

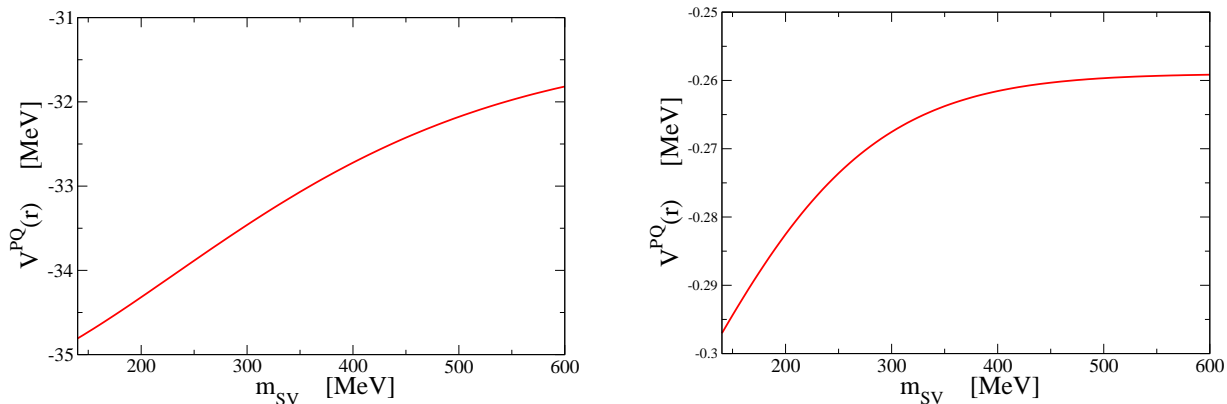


FIG. 4. The left panel shows $V^{\text{PQ}}(r)$ evaluated at $r = 1$ fm as a function of the meson mass m_{SV} , while the right panels shows $V^{\text{PQ}}(r)$ evaluated at $r = 2$ fm. The vertical axis is in units of MeV. When $m_{SV} = m_\pi$ the value of $V^{\text{PQ}}(r)$ is equal to $V^{\text{QCD}}(r)$.

where m_{SV} is the mass of a meson containing one sea quark and one valence quark. In Fig. 4 we show $V^{\text{PQ}}(r)$ evaluated at $r = 1$ fm and $r = 2$ fm as a function of m_{SV} . In contrast to the NN potential that is dominated at long-distances by partial-quenching effects, the $\Lambda_Q\Lambda_Q$ potential receives comparable contributions from both the valence quarks and the ghost quarks, and in fact the (partial) quenching contribution is somewhat smaller than the QCD contribution. When $m_{SV} = m_\pi$ we recover the value of the potential in QCD, as has to be the case.

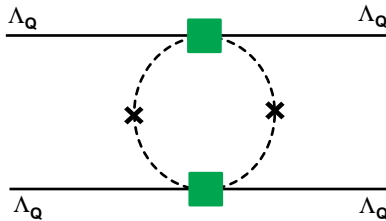


FIG. 5. The leading hairpin contribution to the $\Lambda_Q\Lambda_Q$ potential. The crosses denote double-pole η propagators and the boxes are vertices from Lagrange density in eq. (12)

Given the large hairpin contribution to the NN potential, it is important to estimate the size of the hairpin contribution to the $\Lambda_Q\Lambda_Q$ potential. The Lagrange density for the leading η (hairpin) interactions, neglecting operators involving insertions of the light-quark mass matrix, is

$$\mathcal{L} = \frac{1}{\Lambda_\chi^3} \left[c_1 (\nabla\eta)^2 + c_2 (\partial_0\eta)^2 \right] \bar{\Lambda}_Q\Lambda_Q \quad , \quad (12)$$

where Λ_χ is the chiral-symmetry breaking scale and $c_{1,2}$ are unknown constants whose natural size is $c_{1,2} \sim 1$ by naive dimensional analysis. One finds that two-insertions of the interactions in eq. 12, as shown in Fig. 5, give a contribution to the $\Lambda_Q\Lambda_Q$ potential of

$$V^{\text{HP}}(r) = -\frac{(m_{SS}^2 - m_\pi^2)^2}{32\pi^3 \Lambda_\chi^6} \int_0^\infty d\lambda e^{-2r\sqrt{\lambda^2 + m_\pi^2}} \left[\left(\frac{2}{r^2} + \lambda^2 + m_\pi^2 \right) c_1^2 + 2\lambda^2 c_1 c_2 + c_2^2 \frac{\lambda^4}{\lambda^2 + m_\pi^2} \right]. \quad (13)$$

The remaining integral can be performed analytically in terms of modified Bessel functions and Struve functions, but it is less than illuminating and we do not present it here. This contribution is suppressed compared to the leading non-hairpin contributions as dictated by the EFT power counting. Numerically, we find that the hairpin contribution to the potential at $r = 1$ fm is $V^{\text{HP}}(1 \text{ fm}) \sim -1$ keV, while at $r = 2$ fm is $V^{\text{HP}}(2 \text{ fm}) \sim -0.06$ keV for $c_1 = c_2 = 1$, $\Lambda_\chi \sim 1$ GeV and $m_{SS} = 600$ MeV. At asymptotically large distances the potential becomes

$$V^{\text{HP}}(r) \rightarrow -c_1^2 \frac{(m_{SS}^2 - m_\pi^2)^2 m_\pi^{5/2}}{64 \pi^{5/2} \Lambda_\chi^6} \frac{e^{-2m_\pi r}}{\sqrt{r}} + \dots \quad (14)$$

where the dots represent subleading contributions in the large-distance expansion. While at asymptotically large distances this contribution is larger than that from the box and crossed-box diagrams, asymptopia finally sets in at distances at which all contributions are numerically insignificant.

IV. CONCLUSIONS

In this work we have computed the potential between two Λ_Q 's at leading order in effective field theory in both QCD and PQQCD. Further, we have estimated the size of the leading contribution from hairpin interactions in PQQCD. We find that the partially-quenched $\Lambda_Q \Lambda_Q$ potential does not suffer from some of the (partial-) quenching problems that plague the NN potential due to the absence of single pseudo-Goldstone exchange. The potentials we have computed in this work will allow for the chiral extrapolation of lattice calculations performed with unphysically large sea quark masses.

As these potentials fall off with a mass scale set by $\sim 2m_\pi$, they are quite small for baryon separations greater than $r \sim 1.5$ fm. Therefore, the theoretical advantages of studying this system to learn about the NN potential may be undermined by the difficulties in extracting a signal from lattice simulations. However, the simplifications introduced by only having two light quarks, and a single infinitely-massive quark to fix the inter-baryon separation makes this system a prime candidate for studying inter-baryon interactions. We look forward to the Jlab/MIT group [14] carrying out their program in this area.

ACKNOWLEDGMENTS

We are grateful to Steve Sharpe for providing valuable insight. This work is supported in part by the U.S. Dept. of Energy under Grant No. DE-FG03-97ER4014 (D.A. and M.J.S.) and Grant No. DE-FG03-00-ER-41132 (S.R.B.).

REFERENCES

- [1] V.G. Stoks, R.A. Klomp, C.P. Terheggen and J.J. de Swart, *Phys. Rev.* **C49**, 2950 (1994); R.B. Wiringa, V.G. Stoks and R. Schiavilla, *Phys. Rev.* **C51**, 38 (1995); R. Machleidt, *Phys. Rev.* **C63**, 024001 (2001).
- [2] M.M. Nagels, T.A. Rijken and J.J. de Swart, *Phys. Rev.* **D12**, 744 (1975).
- [3] P.F. Bedaque and U. van Kolck, *Ann. Rev. Nucl. Part. Sci.* **52**, 339 (2002); D.R. Phillips, *Czech. J. Phys.* **B49**, 52 (2002); S.R. Beane, P.F. Bedaque, W.C. Haxton, D.R. Phillips and M.J. Savage, Essay for the Festschrift in honor of Boris Ioffe, in the Encyclopedia of Analytic QCD, At the Frontier of Particle Physics, vol. 1, 133-271, edited by M. Shifman (World Scientific).
- [4] M.C. Rentmeester, R.G. Timmermans, J.L. Friar and J.J. de Swart, *Phys. Rev. Lett.* **82**, 4992 (1999); M.C. Rentmeester, R.G. Timmermans and J.J. de Swart, [nucl-th/0302080](#).
- [5] M. Lüscher, *Commun. Math. Phys.* **105**, 153 (1986).
- [6] R. Gupta, A. Patel and S. R. Sharpe, *Phys. Rev.* **D48**, 388 (1993).
- [7] M. Fukugita, Y. Kuramashi, M. Okawa, H. Mino and A. Ukawa, *Phys. Rev.* **D52**, 3003 (1995).
- [8] D.G. Richards, D.K. Sinclair and D.W. Sivers, *Phys. Rev.* **D42**, 3191 (1990).
- [9] A. Mihaly, H.R. Fiebig, H. Markum and K. Rabitsch, *Phys. Rev.* **D55**, 3077 (1997).
- [10] C. Stewart and R. Koniuk, *Phys. Rev.* **D57**, 5581 (1998).
- [11] C. Michael and P. Pennanen [UKQCD Collaboration], *Phys. Rev.* **D60**, 054012 (1999).
- [12] D.G. Richards, [nucl-th/0011012](#).
- [13] H.R. Fiebig and H. Markum, [hep-lat/0212037](#).
- [14] <http://www.jlab.org/~dgr/lhpc/march00.pdf>;
http://www.jlab.org/~dgr/lhpc/sdac_proposal_final.pdf.
- [15] S.R. Beane and M.J. Savage, *Phys. Lett.* **B535**, 177 (2002).
- [16] S.R. Beane, P.F. Bedaque, M.J. Savage and U. van Kolck, *Nucl. Phys.* **A700**, 377 (2002).
- [17] S.R. Beane and M.J. Savage, *Phys. Rev.* **D67**, 054502 (2003).
- [18] P.L. Cho, *Phys. Lett.* **B285**, 145 (1992); *Nucl. Phys.* **B396**, 183 (1993); Erratum-ibid. **B421**, 683 (1994).
- [19] T.-M. Yan, H.-Y. Cheng, C.-Y. Cheung, G.-L. Lin, Y.C. Yin and H.-L. Yu, *Phys. Rev.* **D46** 1148 (1992).
- [20] K. Hagiwara *et al.* [Particle Data Group Collaboration], *Phys. Rev.* **D66**, 010001 (2002).
- [21] S.R. Beane and M.J. Savage, *Phys. Lett.* **B556**, 142 (2003).
- [22] M. Lu, M.J. Savage and J. Walden, *Phys. Lett.* **B369**, 337 (1996).
- [23] E. Jenkins and A.V. Manohar, *Phys. Lett.* **B255**, 558 (1991).
- [24] T.A. Rijken and V.G. Stoks, *Phys. Rev.* **C46**, 73 (1992).
- [25] G. Chiladze, *Phys. Rev.* **D57**, 5586 (1998).
- [26] J.N. Labrenz and S.R. Sharpe, *Phys. Rev.* **D54**, 4595 (1996); M.J. Savage. *Nucl. Phys.* **A700** 359 (2002); J.-W. Chen and M.J. Savage, *Phys. Rev.* **D65**, 094001 (2002); S.R. Beane and M.J. Savage, *Nucl. Phys.* **A709**, 319 (2002).